Chemical trends for deep levels associated with vacancy-impurity complexes in semiconductors

Yu-Tang Shen*
Department of Physics, University of Texas at Austin, Austin, Texas 78712

Charles W. Myles
Department of Physics and Engineering Physics, Texas Tech University, Lubbock, Texas 79409
(Received 15 February 1989)

A theory of the deep levels produced by triplet vacancy-impurity complexes in covalent semiconductors is presented. The major chemical trends in the deep levels of a_1 and b_1 symmetry are predicted for such complexes in 10 materials. These calculations show that a triplet vacancy-impurity complex can produce deep levels at energies where neither the corresponding vacancy-impurity pair nor the isolated impurity produce any.

I. INTRODUCTION

The performance characteristics of semiconductor devices can be altered by defects in the device material. In particular, defect energy levels in the band gap can greatly influence the material electrical and optical properties. These levels fall into the two general classes of shallow levels, which are usually formed by defects whose valence differs from that of the host by unity,[1] and "deep" levels,[2–7] which lie well within the band gap. Shallow levels are produced by the long-ranged Coulomb potential of the defect and lie within about 0.1 eV from a band edge. By contrast, deep levels are controlled by the central-cell, atomiclike potential of the defect. Hjalmarson, Vogl, Wolford, and Dow[7] have shown that the chemical trends in the deep levels of substitutional impurities can be understood using a Koster-Slater[8] model where only the central-cell part of the defect potential is treated, and where this potential is modeled by the assumption that it is proportional to the atomic-energy differences of the defect and host atoms. Sankey and co-workers[9–13] have generalized these ideas to treat paired impurities, and have predicted the chemical trends in the deep pair levels in several materials. The latter theory was modified by Myles and Sankey,[14] who treated vacancy-impurity pairs and predicted the chemical tends in the deep levels due to such defects in twelve materials.

In the present paper, we present a simple theory[15] of the deep levels associated with triplet complexes in covalent semiconductors and present predictions for the major chemical trends in the levels of a_1 and b_1 symmetry for such complexes in 10 materials. The terminology "triplet complex" is used to denote a vacancy-impurity complex consisting of a vacancy that is a nearest neighbor to two identical, substitutional sp^3-bonded impurities. This type of defect is the simplest possible vacancy-impurity complex containing three constituents. The results of the application of our theory to triplet complexes in GaAs and GaP have been presented earlier.[16] It is the purpose of the present paper to present a more detailed discussion of our theory, to apply it to other materials, and to make comparisons with available data.

The motivation for considering vacancy-complex produced deep levels is that vacancies are important native defects in semiconductors and are present to some extent, regardless of the material-preparation technique. Furthermore, they are mobile and can migrate and be trapped by impurities to form complexes. These complexes have been shown to have important effects on the efficiency of radiative recombination in a number of materials such as Si,[17] GaP,[18] GaAs,[19] $GaAs_{1-x}P_x$,[20] ZnTe,[21] ZnSe,[22] and $Hg_{1-x}Cd_xTe$.[23]

Our theory is based on the theory of Hjalmarson *et al.* of deep levels[7,24] and on the semiempirical sp^3s^* tight-binding band-structure model of Vogl *et al.*[25] The theory[7,24] of Hjalmarson *et al.* and various generalizations of it, when used with the band structures of Vogl *et al.*[25] have been successful in their predictions of chemical trends in the bulk[9–16,26–28] and surface[29] defect-related properties of numerous semiconductor materials. Furthermore, generalizations of this theory have often produced results which are in semiquantitative agreement, both with experiment[9–16,26–29] and with more sophisticated theories.[28] Theoretical uncertainties for the absolute energy levels predicted by this theory are typically a few tenths of an electron volt, in comparison with either data or other calculations (which often have comparable uncertainties). However, the chemical trends predicted by this approach have usually been shown to be correct, in cases where they could be checked. For instance, Hjalmarson's[7] early predictions for the trends of isolated acceptor levels in Si are in agreement with data, but the experimental binding energy for the deep In acceptor in Si is not accurately predicted. In fact, Hjalmarson predicts that this level should be valence-band resonant.

Some specific cases where the chemical trends obtained using generalizations of the theory of Hjalmarson *et al.*[7,24] have been found to be in quite good agreement with experiment are the following: (1) the predictions by Sankey *et al.*[9] of the x dependences of the deep levels associated with the Ga-vacancy–O pair and the Zn-O pair

in $GaAs_{1-x}P_x$, (2) the calculations by Sankey and Dow for the deep levels due to pairs of impurities in GaAs,[10] InP,[11] and Si,[13] (3) the results of Dow *et al.*[12] for core-exciton binding energies in III-IV compound semiconductors, (4) the predictions by Myles and Sankey[14] of the deep levels due to vacancy-impurity pairs in GaAs, GaP, and GaSb, (5) the calculations of Myles *et al.*[23] of the x dependences of the deep levels produced by cation-vacancy–associated complexes in $Hg_{1-x}Cd_xTe$, (6) the results of Ford *et al.*[26] for the alloy composition dependence of the inhomogeneous broadening of various deep levels in $GaAs_{1-x}P_x$, $Al_xGa_{1-x}As$, and $Hg_{1-x}Cd_xTe$, (7) the predictions of Lee *et al.*[28] for the charge-state splittings of deep levels due to chalcogen impurities in Si, and (8) the results of Allen *et al.*[29] of the Fermi-level-pinning energies produced by deep levels due to anisite defects at the surfaces of semiconductor alloys. The latter results correlate well with the alloy composition dependences of the Schottky-barrier heights at the interfaces of such alloys with various metals.

Quantitative comparisons of the absolute energy levels resulting from the approach of Hjalmarson *et al.*[7,24] and its generalizations, either with data or with other theoretical calculations, yield discrepancies ranging from less than 0.1 eV to several tenths of an electron volt. Agreement to within less than 0.1 eV is considered fortuitous, given the expected uncertainty in the absolute energy predictions. Examples of the ranges of quantitative agreement expected between the results of this approach and experimental data are as follows: (1) the deep pair levels in $GaAs_{1-x}P_x$ obtained by Sankey *et al.*,[9] for which theory and experiment agree for all x to within about 0.02 eV for the Zn-O pair and about 0.1 eV for the Ga-vacancy–O pair; (2) the Schottky-barrier heights predicted by Allen *et al.*[29] for gold-semiconductor alloy interfaces, for which theory and experiment disagree by about 0.3 eV for all x in $Al_xGa_{1-x}As$ and $GaAs_{1-x}P_x$ and agree to within less than 0.1 eV for $x>0.3$ in $In_xGa_{1-x}P$ and for $x<0.7$ in $Ga_xIn_{1-x}As$; and (3) the deep levels and charge-state splittings of neutral and singly positively charged chalcogens in Si, obtained by Lee *et al.*[28] In the latter case, theory and experiment differ by 0.31, 0.37, 0.30, 0.37, 0.19, and 0.21 eV for deep levels due to S^0, S^+, Se^0, Se^+, Te^0, and Te^+, and they agree to within 0.07, 0.07, and 0.02 eV for the charge-state splittings between the levels produced by S^0 and S^+, Se^0 and Se^+, and Te^0 and Te^+, respectively.

On the basis of its past performance, as outlined in the preceding paragraphs and as discussed in greater detail in many places in the literature,[7,9–16,23–29] we have confidence that this theory can predict the major chemical trends in the energies of triplet complex levels in the materials we consider here. However, also based on this performance, we expect that the uncertainties in the absolute energy levels we predict can be as large as a few tenths of an electron volt. Thus, the absolute numbers obtained by our theory should not be taken as seriously as the chemical trends which emerge from it.

Our theory is the next logical step in the treatment of vacancy-impurity complexes beyond the Myles-Sankey[14] theory of vacancy-impurity pairs. Following Ref. 14, our primary interest is in obtaining chemical trends in the deep levels due to triplet complexes. To this end, we consider only such complexes which contain an ideal vacancy.[30]

Our principal finding is that a triplet complex can produce deep levels which are significantly altered in comparison with those produced by either the vacancy-impurity pair[14] or the isolated impurity.[7,24] Thus, the presence of vacancies in a material can greatly alter the positions of the deep levels associated with particular impurities. Our predictions of vacancy-complex–associated levels will hopefully serve as a guide to experimentalists attempting to interpret data.

II. THEORY

The perfect-crystal Hamiltonian we use is the sp^3s^* nearest-neighbor tight-binding model of Vogl *et al.*,[25] which has five states per atom (the four sp^3 states and an excited s^* state) with 13 parameters that were obtained by an empirical fit to pseudopotential band structures.[31] The parameters describing this Hamiltonian can be found in Ref. 25. The use of an excited s^* state enables a description of the conduction bands that is flexible enough to treat both direct- and indirect-band-gap semiconductors. This model successfully reproduces the principal features of the lower conduction-band structure of several materials.[25]

The Hamiltonian of Vogl *et al.*[25] has the form

$$H_0=\sum_{i,\mathbf{R}}(|ia\mathbf{R}\rangle E_i^a\langle ia\mathbf{R}|+|ic\mathbf{R}\rangle E_i^c\langle ic\mathbf{R}|) + \sum_{\substack{i,j\\ \mathbf{R},\mathbf{R}'}}(|ia\mathbf{R}\rangle V_{ij}(\mathbf{R},\mathbf{R}')\langle jc\mathbf{R}'|+\text{H.c.}), \quad (1)$$

where $i=s$, p_x, p_y, p_z, or s^* labels the orbitals, a and c refer to the anion and cation, $\mathbf{R}$ labels the unit cell, and H.c. denotes the Hermitian conjugate. The transfer-matrix elements V_{ij} are nonzero only between nearest neighbors; when $|\mathbf{R}+\mathbf{d}-\mathbf{R}'|=|\mathbf{d}|$, where $\mathbf{d}$ is the nearest-neighbor vector, $\mathbf{d}=a_L(1,1,1)/4$. Here, a_L is the cubic lattice constant. The states $|ia\mathbf{R}\rangle$ and $|ic\mathbf{R}\rangle$ are localized basis orbitals centered on the anion at $\mathbf{R}+\mathbf{d}$ and on the cation $\mathbf{R}$, respectively. The tight-binding parameters of H_0 have the property that differences of the on-site matrix elements E_i are proportional to the corresponding atomic energy differences of the host atoms[32] and the nearest-neighbor transfer-matrix elements V_{ij} scale roughly according to Harrison's $|\mathbf{d}|^{-2}$ rule.[32]

A schematic diagram of the type of defect we consider is shown in Fig. 1. This figure shows a triplet complex of nearest-neighbor impurities in the unit cell at $\mathbf{R}=\mathbf{0}$. This complex consists of an impurity at the center of the unit cell, taken to be on the cation site for definiteness, complexed with two other impurities which are identical to each other. In this figure the circles with crosses denote host atoms, the hatched circle denotes a cation impurity at the origin (to be replaced by a vacancy), and the two open circles denote anion impurities. Occupying anion sites 1 and 2 are two identical impurity atoms with site indices $\mathbf{d}$ and $\mathbf{d}'$, respectively, where $\mathbf{d}'$

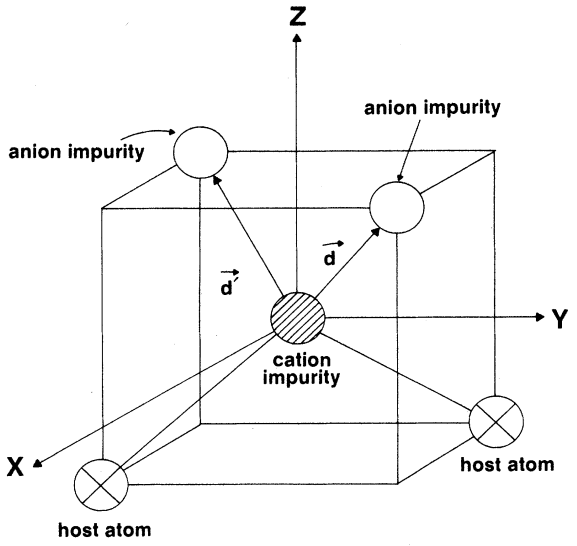

FIG. 1. Schematic diagram of a triplet impurity complex. The circles with crosses denote the host atoms, the hatched circle denotes the cation at the origin, and the two open circles denote two identical impurity atoms which occupy the sites **d** and **d'**, respectively.

$=a_L(-1,-1,1/4)$ This figure illustrates a more general case than we consider here, and much of the formalism outlined here and in Ref. 15 can therefore be used to treat complexes consisting of three impurities. However, here we consider only triplet complexes containing a vacancy at the central site and take the limit as the defect potential of the central-site impurity approaches that of a vacancy. In Fig. 1 and in our formalism, we explicitly consider the case where the origin is taken to be the cation site. The opposite case, where the origin is the anion site and the impurity occupying it is replaced by a vacancy, can also be easily treated by interchanging anion and cation labels in all equations. Thus, in the results presented below, we consider triplet complexes containing both cation and anion vacancies.

We follow Hjalmarson *et al.*[7] in constructing the defect potential. For the impurity sites of the complex (anion sites 1 and 2 in Fig. 1), the on-site matrix elements are obtained from the atomic-energy differences of the impurity and the host, and the off-diagonal matrix elements are taken to be zero. For the vacancy site of the complex (the cation site in Fig. 1), we take the diagonal matrix elements of the defect potential to be infinite and the off-diagonal matrix elements to be zero. An infinite potential has been used to model an ideal vacancy in numerous previous studies.[14–16,30] This approximation allows the vacancy "atom" to be decoupled from the host and simulates the effect of a missing atom.

With these assumptions, the defect potential for the triplet complex is diagonal in the tight-binding basis, but properly accounts for the defect chemistry.[7] Both charge-state splittings and lattice relaxation are neglected in this theory. The neglect of lattice relaxation around a vacancy would be a serious omission if one desired precise predictions of absolute trap depths. However, the neglect of such effects in a theory of chemical trends has been justified in previous work,[7,9–16] where it is argued that they tend to be monotonic functions of trap depth. The neglect of them is therefore not expected to greatly alter the *ordering* of the predicted deep levels. The resulting theory gives a global view of chemical trends, but as is discussed above, it is limited by uncertainties as large as a few tenths of an electron volt. The long-ranged, dielectrically screened Coulomb potential is also neglected because it has a small effect on the energy scale of interest, so that shallow impurities have zero binding energy in this model. The theory can, in principle, be modified to include these neglected effects.[28]

For the defect illustrated in Fig. 1, the above assumptions allow the defect potential to be written as

$$U=\sum_i(|ic\mathbf{0}\rangle U_i^c\langle ic\mathbf{0}|+|ia\mathbf{d}\rangle U_i^a\langle ia\mathbf{d}| + |ia\mathbf{d}'\rangle U_i^a\langle ia\mathbf{d}'|)\ , \tag{2}$$

where U_i^c and U_i^a are the cation- and anion-site defect potentials for orbital i. For a similar defect with the anion site at the origin, the labels a and c are interchanged in Eq. (2). In Eq. (2) the sum over i is only over the s, p_x, p_y, and p_z orbitals, following previous work.[7–16,33] Also following previous work, we assume that all orientations of the p orbitals have the same defect-potential energies. Thus, there are only four independent parameters in the defect potential: U_s^c, U_p^c, U_s^a, and U_p^a. Following Hjalmarson *et al.*,[7] for the impurity sites of the complex, we take each of these parameters to be proportional to an appropriate difference between defect and host atomic energies.[34] For the case of interest here, where the central site is occupied by an ideal vacancy,[30] we take the appropriate defect potential matrix element to be infinite.[30] For a cation (anion) vacancy we thus take U_i^c (U_i^a)$\rightarrow\infty$. in Eq. (2).

The defect potential in Eq. (2) is local in the tight-binding basis, so that the Koster-Slater theory[8] is convenient for determining the bound-state energies E of the triplet complex. In this method, these energies are given by solutions to the determinantal equation

$$\det[I-G^0(E)U]=0\ , \tag{3}$$

where

$$G^0(E)=(E-H_0)^{-1} \tag{4}$$

is the host Green's function, and I is the identity matrix. The advantage of this method is that the determinant in Eq. (3) only needs to be evaluated in the subspace of U. In the present case, this yields a 12×12 determinant (three sites and four orbitals—one s and three p—per site).

It should be pointed out that, for isolated impurities[7,24] and paired defects,[9–14] the block diagonalization of the host Green's function was relatively straightforward because of the high symmetry of the defects. In the present case, however, the defect symmetry is reduced and block

diagonalization is nontrivial. The determinant in Eq. (3) can, however, still be somewhat simplified by symmetry considerations.[35] The point group for a point defect in a zinc-blende semiconductor is T_d. Point defects with sp^3 hybrid bonding can thus have defect states with either nondegenerate A_1 (s-like) or triply degenerate T_2 (p-like) symmetry. Triplet complex defects in the same host are described by a reduced "molecular" symmetry group C_{2v} (Ref. 35) (a twofold axis of rotation and two reflection planes containing the twofold axis and perpendicular to each other). This results in splittings of the T_2 levels and mixing of the "atomic" A_1 and T_2 levels on the three sites.[35] Due to the fact that the point group C_{2v} has one-dimensional irreducible representations only,[35] the T_2 level is split into three nondegenerate levels. The resulting "molecular" states are denoted as a_1-symmetric (s,p_z-like), b_1-symmetric (p_x-like), and b_2-symmetric (p_y-like). The a_1 and b_2 orbitals result from the strong overlap and mixing of the A_1 levels and the p_x and p_z components of the T_2 levels on the three sites. Thus, their energies may be very unlike those of either the isolated impurity or the isolated vacancy. Therefore, they are the most interesting of the triplet complex levels. On the other hand, the b_2 states correspond to admixtures of the p_y orbitals on the three sites. Since these mix only weakly due to the orientation of the complex, the corresponding levels are relatively unaffected by complexing and are very close to both the levels of the T_2 states of the isolated defects[7,24] and those of the e-symmetric levels of the corresponding vacancy-impurity pair.[14] Due to this fact, results for the b_2 levels will not be presented here.

In the subspace of the defect defined by Eq. (2), the host Green's function is a 12×12 matrix. After using the symmetric operations of the point group C_{2v} (Ref. 35) to block-diagonalize this matrix into the direct sum of four smaller matrices, and after using the same operations on the defect potential, Eq. (3) factors to become the product of four smaller determinants,[15]

$$\det[I_5-G_5^0(E)U_5]\det[I_4-G_4^0(E)U_4]\det[I_2-G_2^0(E)U_2]\det[I_1-G_1^0(E)U_1]=0\ , \tag{5}$$

where $G_i^0(E)$, U_i, and I_i are, respectively, the Green's-function submatrix, the defect-potential submatrix, and the unit matrix of size $i\times i$ ($i=1,2,4,5$) that result from these operations. The defect-potential matrices U_i remain diagonal in this representation. The details of the block diagonalization of $G^0(E)$ and the factoring of Eq. (3) to give Eq. (5) are discussed in Ref. 15 and are summarized in the Appendix. The matrix elements of $G_i^0(E)$, shown in the Appendix, are linear combinations of the matrix elements of $G^0(E)$ in the tight-binding basis. An important feature of these matrix elements is that, since they are evaluated using only the unperturbed Hamiltonian, they depend only on the host band structure. Also, because the matrix elements of G^0 are between localized orbitals, they include contributions from all of k space and from energetically distant bands. It is also worthwhile pointing out that, even though the matrix elements of the unperturbed Hamiltonian H_0 are nonzero only between nearest neighbors in the present model, this is *not* true for the matrix elements of G^0. For example, such matrix elements between localized states on second-nearest-neighbor atoms are nonzero and the inclusion of them is vital in the calculations outlined above.

For the case where the cation (anion) site at the origin is occupied by a vacancy, we take the limits U_s^c (U_s^a) and U_p^c (U_p^a)$\rightarrow\infty$. This is accomplished numerically, by allowing these quantities to become sufficiently large numbers in Eq. (5). In the results presented below, we have employed Hjalmarson's empirical rule[7,24] that, for the impurity sites of the complex, the diagonal p matrix elements of the impurity potential U_p are equal to one-half of the appropriate diagonal s matrix elements U_s. This simplification is not necessary to solve Eq. (5), but is both helpful for simplifying the computation and consistent with previous uses of the approach of Hjalmarson *et al.*[7,9–16,23,24,26–28] In this approximation, the deep-level energies depend on only one parameter: U_s for the anion or the cation, depending on the case of interest. Justification for this empirical rule may be found in Hjalmarson's dissertation.[24]

It is also worth noting that predictions for the isolated cation or anion vacancy levels can be obtained in our formalism by setting the impurity potentials for the appropriate sites equal to zero. These isolated vacancy deep levels are identical to those obtained by Hjalmarson *et al.*[7,24] Finally, we note in passing that the case of the trivacancy can also be obtained in our formalism by taking the limit as the appropriate impurity potentials approach infinity.

III. RESULTS AND DISCUSSION

A. General discussion of results

We have calculated the deep levels associated with triplet complexes in Si, Ge, GaSb, AlP, AlAs, InP, InAs, InSb, ZnSe, and ZnTe.[15] The results for GaAs and GaP have been presented previously.[16] By exchanging anion and cation labels in our formalism, we have done such calculations for both cation-vacancy and anion-vacancy complexes. We seek the major chemical trends in the ordering of the levels. Due to the neglect of lattice relaxation and charge-state-splitting effects, our results for absolute level depths associated with specific complexes should be viewed on a coarse scale of several tenths of an electron volt. However, based on past successes of similar approaches,[7,9–16,23,26–29] we believe that the ordering we predict for the deep levels as the impurity in the com-

plex is changed should generally be correct.

It should be pointed out, however, that in cases where two predicted levels, either for the same defect or two different defects, occur within a few tenths of an electron volt of each other, the inclusion of such charge-state splitting and lattice-relaxation effects, which are typically of this order of magnitude,[28] could alter the ordering of the two levels. It should also be noted that because each level due to a triplet complex is orbitally nondegenerate, it can be occupied by, at most, two electrons, one for each possible spin orientation. Clearly, in general, the occupancy of such a level (whether it contains zero, one, or two electrons) can affect its position in the band gap. Because of the neglect of charge-state-splitting effects and other electron-electron interactions, however, our theory cannot distinguish between unoccupied, partially occupied, and completely occupied orbital levels.

The results for the a_1- and b_1-symmetric levels obtained from the solution to Eq. (5) are summarized in Figs. 2–11. The figure numbers which display the results for the various materials are Si, Fig. 2; Ge, Fig. 3; GaSb, Fig. 4; AlP, Fig. 5; AlAs, Fig. 6; InP, Fig. 7; InAs, Fig. 8; InSb, Fig. 9; ZnSe, Fig. 10; and ZnTe, Fig. 11. For the compound semiconductors, the (a) parts of the figures correspond to the case of a cation vacancy complex, while the (b) parts correspond to the case of an anion vacancy complex. For comparison, the A_1-symmetric deep levels for the corresponding isolated impurity[7,24] are also shown in these figures (dashed curves). These results also should be compared to the appropriate figures for deep levels produced by vacancy-impurity pairs.[14] In Figs. 2–11 the zero of energy on the vertical scale corresponds to the top of the valence band, and the horizontal scale and the labeled impurities on the top of the figures correspond to the s defect potential of the impurity, from atomic-energy differences.[7,24] The zero of potential on the horizontal scale is the s potential of the anion or cation, as is appropriate.

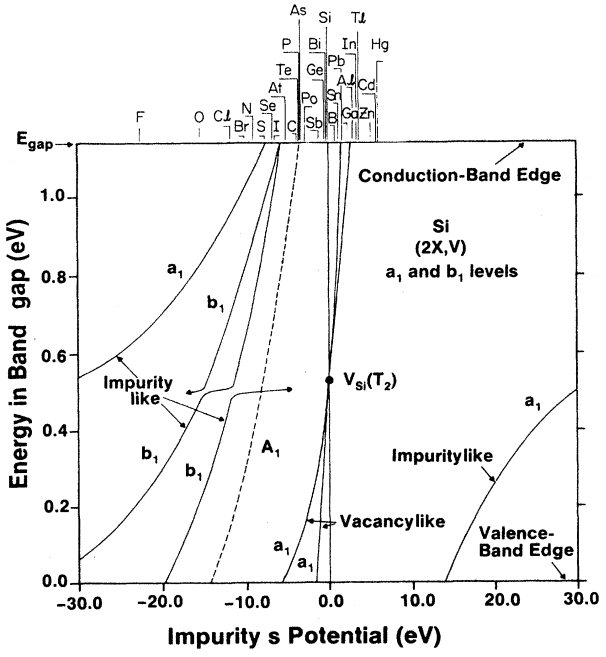

FIG. 2. Energy levels of a_1 and b_1 symmetries produced by a triplet complex $(2X, V)$ associated with a vacancy V and two identical impurities X in Si (solid curves). The abscissa is the s-orbital potential of the impurity X. In this and subsequent figures, the ordinate is the band-gap energy with the zero equal to the top of the valence band. The sp^3-bonded impurities are shown at the top of the figure at their corresponding impurity potentials. For comparison, the A_1-symmetric levels produced by an isolated impurity X (Refs. 7 and 24) are shown as dashed curves.

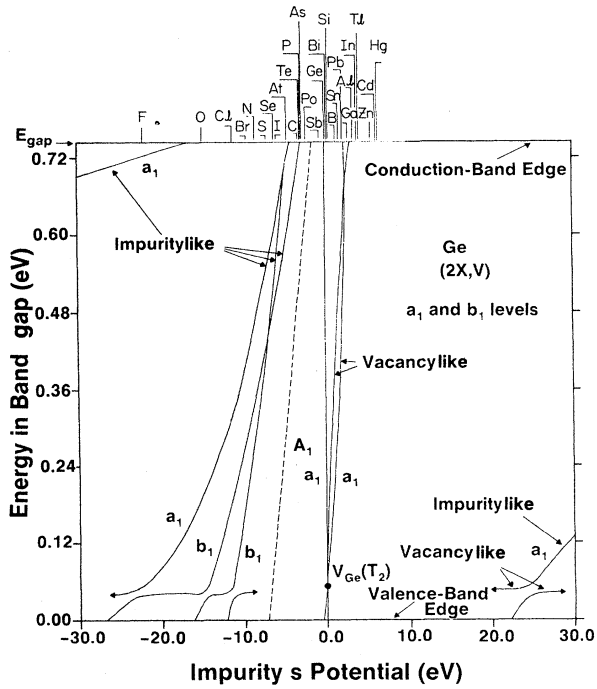

FIG. 3. Energy levels of a_1 and b_1 symmetries produced by a triplet complex $(2X, V)$ in Ge. The remainder of the interpretation is as in Fig. 2.

The deep levels for a particular triplet complex are obtained from these figures by finding the intersection with the appropriate curve of a vertical line drawn from the label for the appropriate impurity at the top of the figure. If there is no such intersection, no deep level is predicted for the complex containing that impurity. The special case of an isolated vacancy can also be found from these figures by allowing the impurity atoms to become host atoms. The resulting predicted isolated vacancy levels[7,24] are shown in Figs. 2–11 as solid circles with appropriate labels. There are two varieties of levels for a given complex (although, one or both could be a band-resonant state). One type has a wave function derived mainly from the impurity, while the other type has a wave function derived mainly from the vacancy. These will be referred to as impuritylike and vacancylike levels, respectively. In some cases hybridization effects can produce substantial mixing of these two types of levels. In interpreting Figs. 2–11 we again call the reader's attention to the fact that

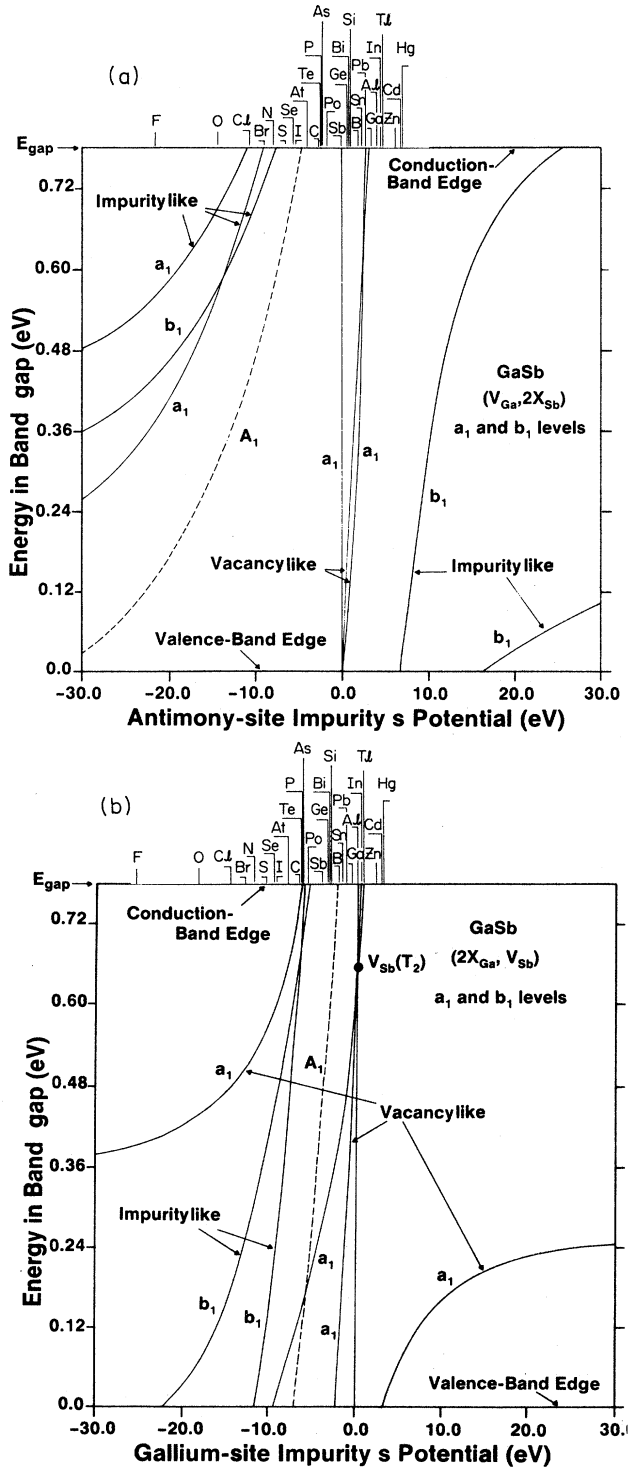

FIG. 4. Energy levels of a_1 and b_1 symmetries produced by triplet complexes in GaSb (solid curves). (a) Levels produced by complexes (V_{Ga}, $2X_{Sb}$) containing a cation (Ga-site) vacancy V_{Ga} and two identical anion (Sb-site) impurities X_{Sb}. (b) Levels produced by complexes ($2X_{Ga}$, V_{Sb}) containing an anion (Sb-site) vacancy V_{Sb} and two identical cation (Ga-site) impurities X_{Ga}. For comparison, A_1-symmetric levels produced by the appropriate isolated impurities X_{Sb} [in (a)] and X_{Ga} [in (b)] are shown in dashed curves (Refs. 7 and 24). The remainder of the interpretation is as in Fig. 2.

the ordering of two closely spaced levels could be reversed by lattice-relaxation or charge-state-splitting effects and that level-occupancy effects could shift some of the predicted levels.

The positions of the triplet-complex-associated a_1- and b_1-symmetric levels with respect to the appropriate iso-

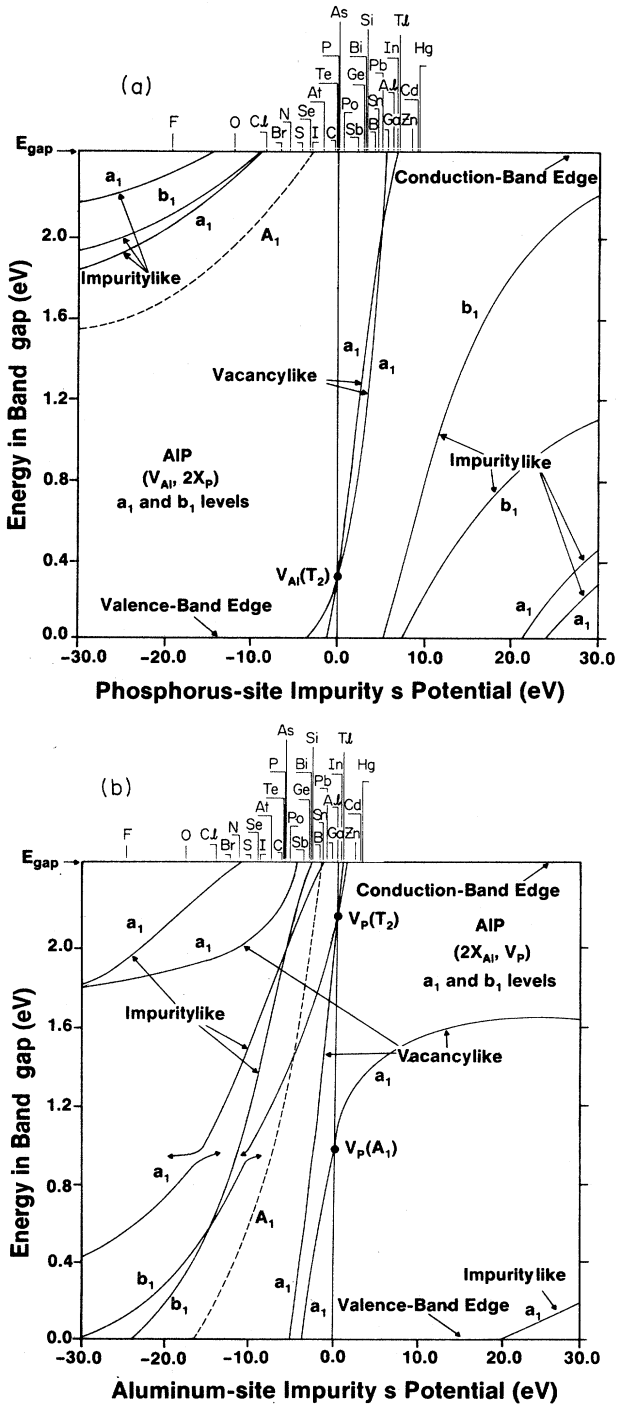

FIG. 5. Energy levels of a_1 and b_1 symmetries produced by triplet complexes in AlP. (a) (V_{Al}, $2X_P$) associated levels. (b) ($2X_{Al}$, V_P) associated levels. The remainder of the interpretation is as in Fig. 4.

lated impurity levels and the similarity between the triplet-complex b_2 levels and the T_2 levels of the isolated impurity can qualitatively be understood by reviewing the vacancy-impurity–pair case and generalizing the discussion to the triplet-complex case. For the vacancy-impurity pair (which has C_{3v} symmetry), as is discussed

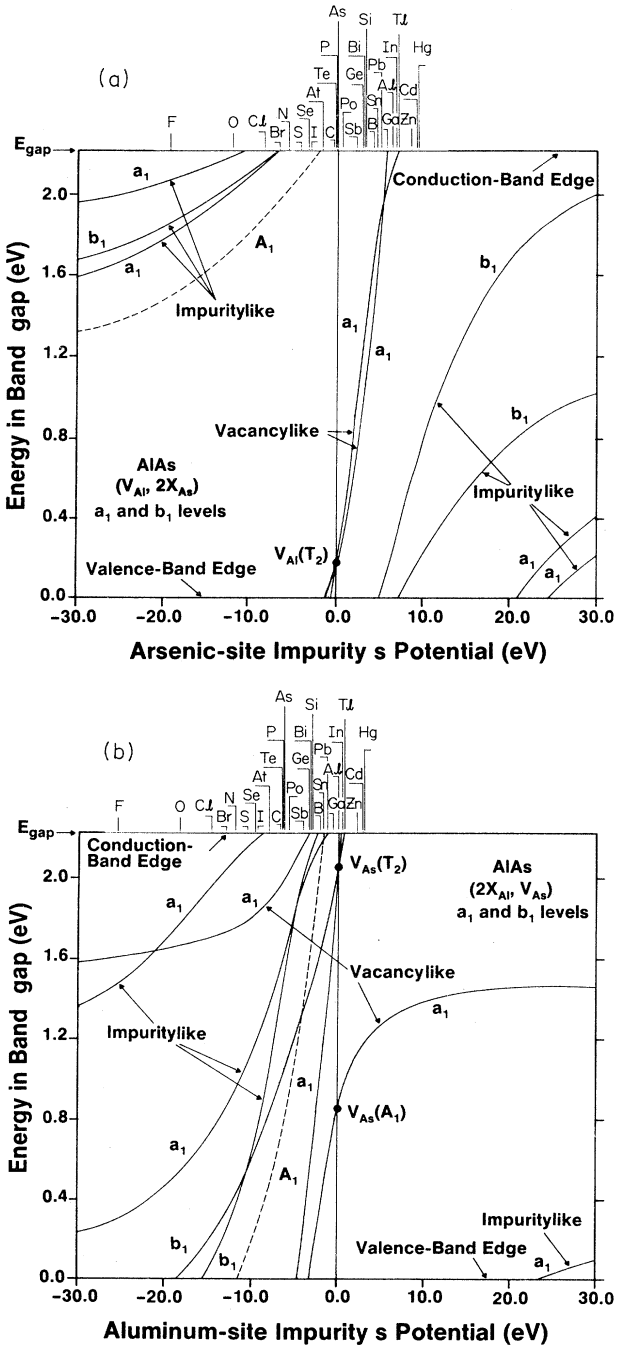

FIG. 6. Energy levels of a_1 and b_1 symmetries produced by triplet complexes in AlAs. (a) (V_{Al},$2X_{As}$) associated levels. (b) ($2X_{Al}$,V_{As}) associated levels. The remainder of the interpretation is as in Fig. 4.

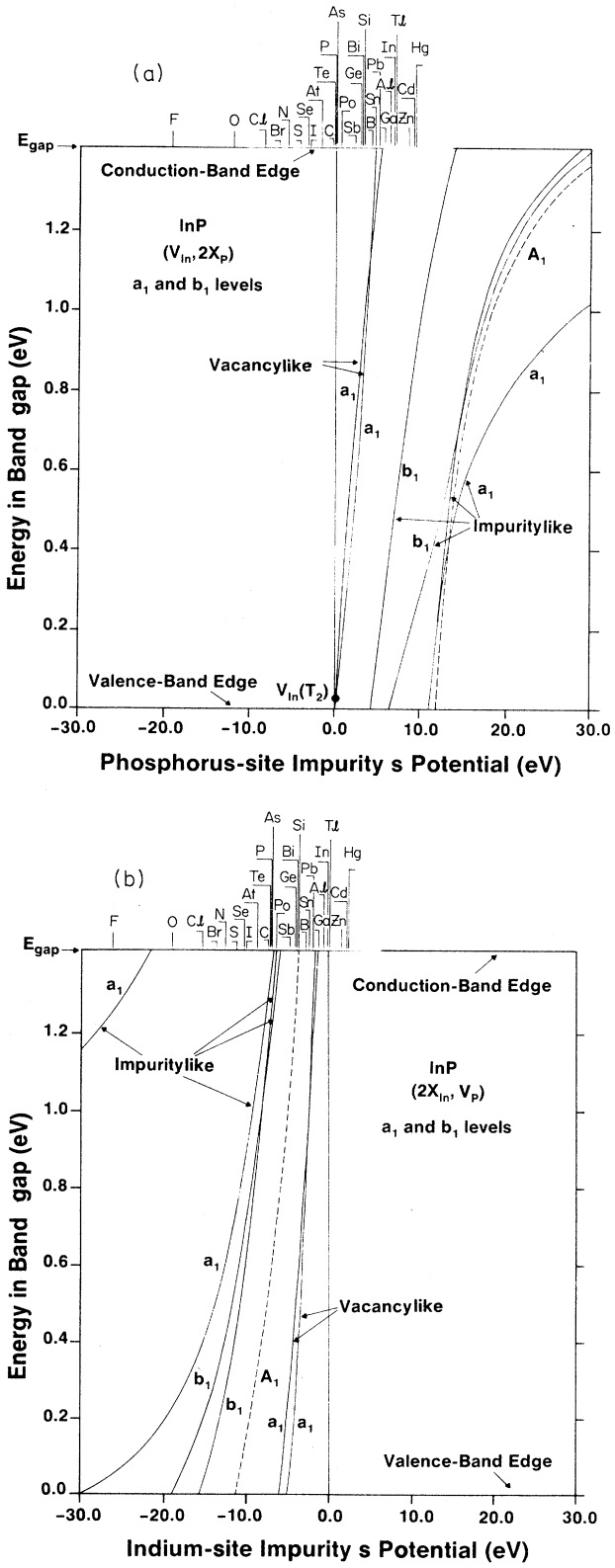

FIG. 7. Energy levels of a_1 and b_1 symmetries produced by triplet complexes in InP. (a) (V_{In},$2X_P$) associated levels. (b) ($2X_{In}$,V_P) associated levels. The remainder of the interpretation is as in Fig. 4.

by Myles and Sankey,[14] σ-like, a_1-pair levels are constructed by mixing the s-like A_1 and p-like T_2 states of both isolated defects. Because this mixing is strong, for σ-like states, these levels may be at different energies than the A_1 or T_2 levels of either isolated defect. However, the π-like, doubly degenerate, e-symmetric levels of the pair have virtually identical energies to those of the impurity and vacancy T_2 levels[14] because they are constructed by mixing the p-like T_2 orbitals of the isolated defects and this mixing is much weaker than for the a_1 levels. Now, let us consider what happens when a second

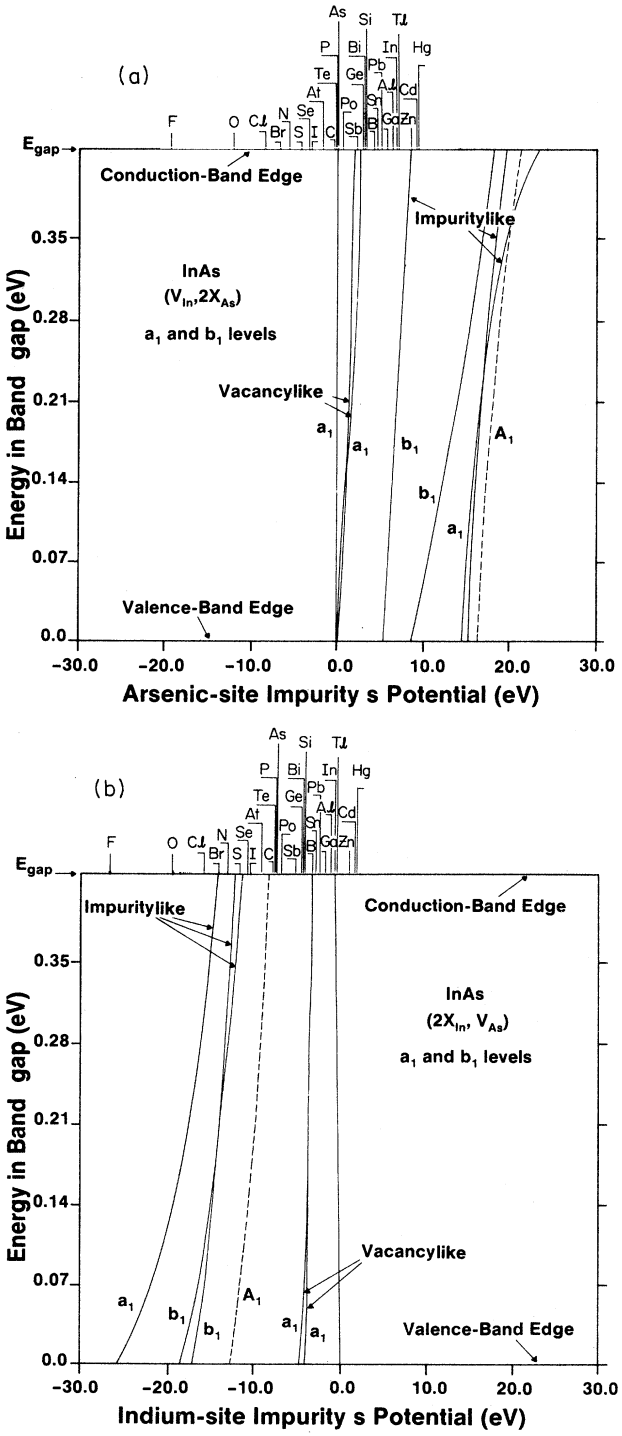

FIG. 8. Energy levels of a_1 and b_1 symmetries produced by triplet complexes in InAs. (a) (V_{In},$2X_{Sb}$) associated levels. (b) ($2X_{In}$,V_{An}) associated levels. The remainder of the interpretation is as in Fig. 4.

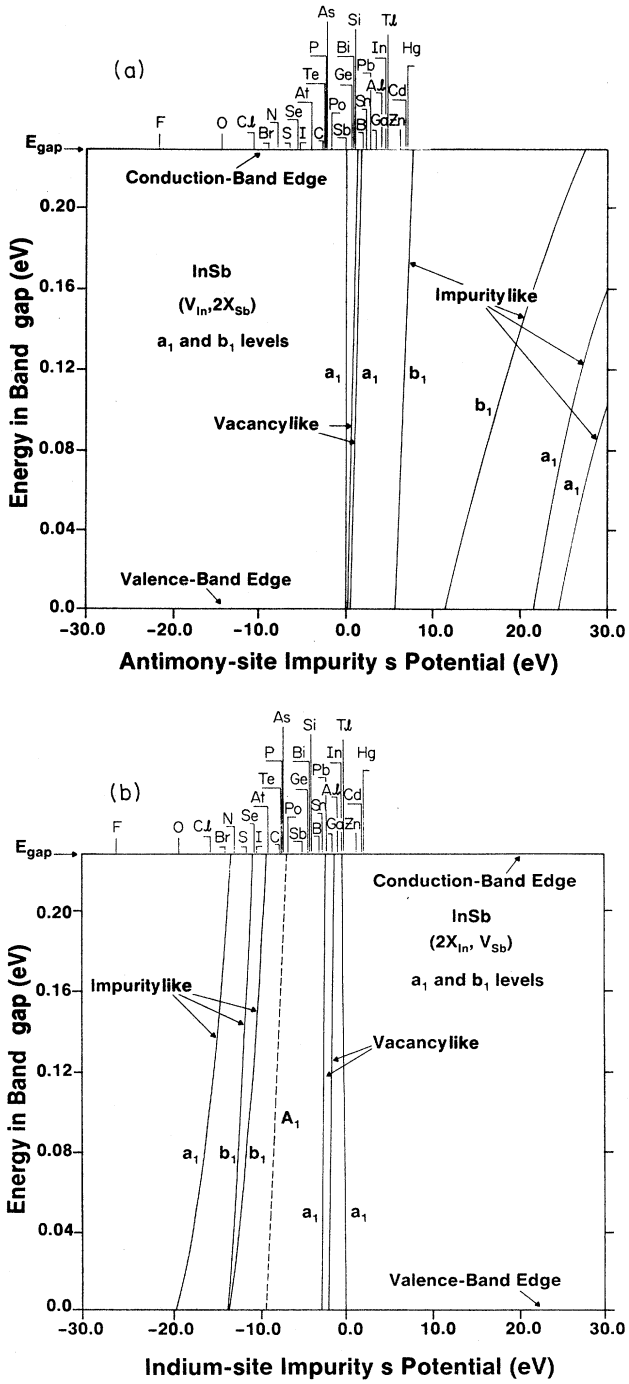

FIG. 9. Energy levels of a_1 and b_1 symmetries produced by triplet complexes in InSb. (a) (V_{In},$2X_{Sb}$) associated levels. (b) ($2X_{In}$,V_{Sb}) associated levels. The remainder of the interpretation is as in Fig. 4.

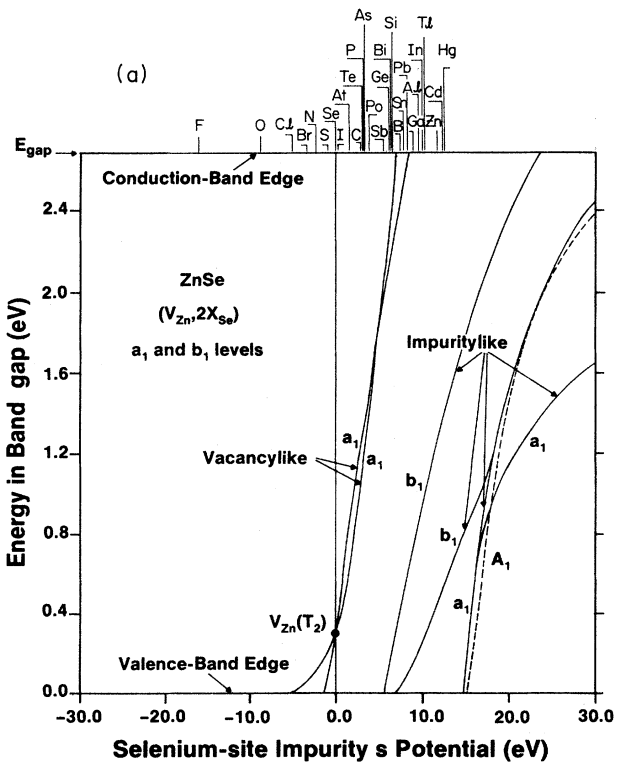

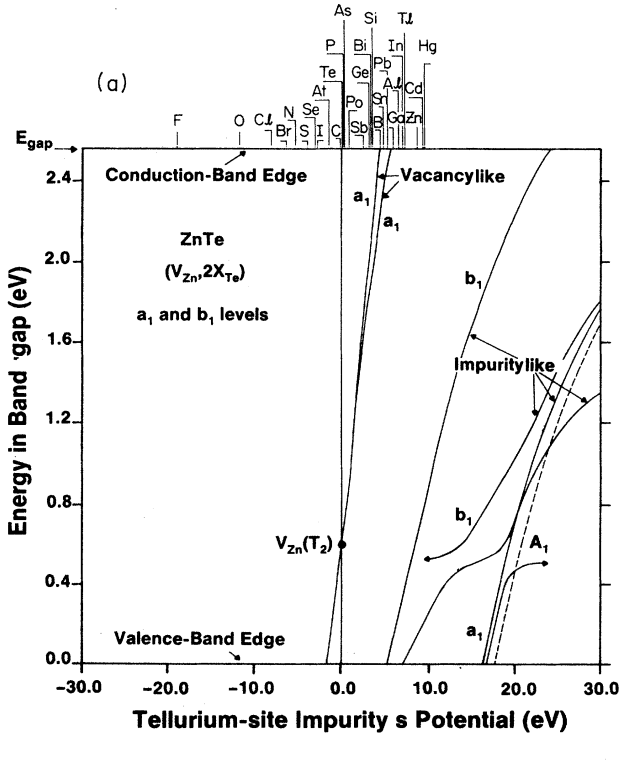

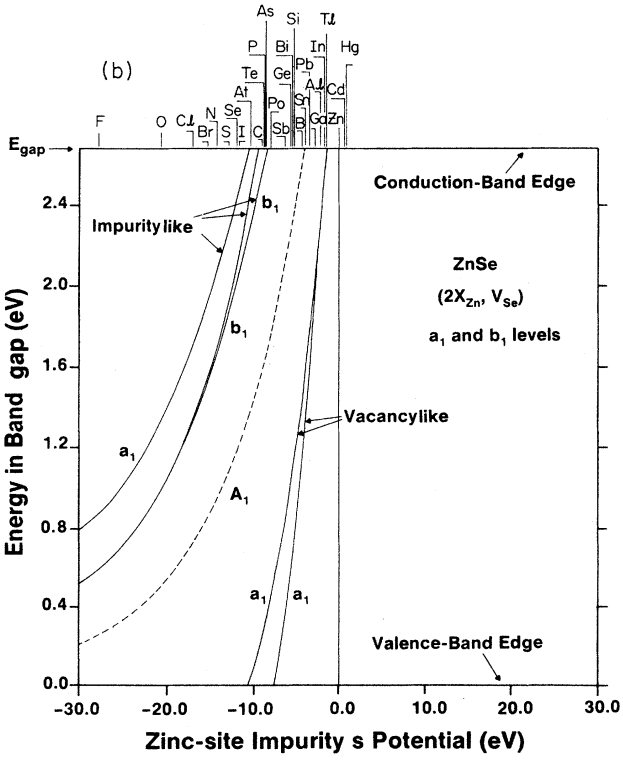

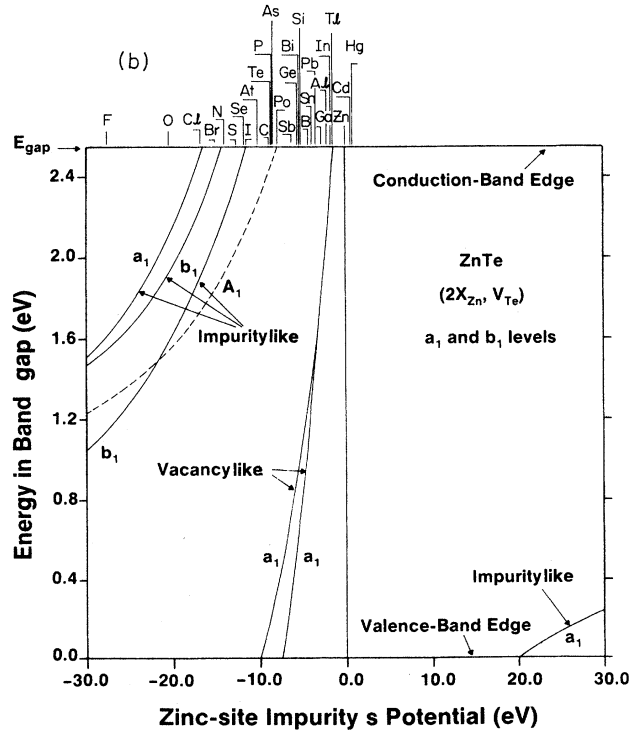

FIG. 10. Energy levels of a_1 and b_1 symmetries produced by triplet complexes in ZnSe. (a) $(V_{Zn},2X_{Se})$ associated levels. (b) $(2X_{Zn},V_{Se})$ associated levels. The remainder of the interpretation is as in Fig. 4.

FIG. 11. Energy levels of a_1 and b_1 symmetries produced by triplet complexes in ZnTe. (a) $(V_{Zn},2X_{Te})$ associated levels. (b) $(2X_{Zn},V_{Te})$ associated levels. The remainder of the interpretation is as in Fig. 4.

impurity is added to the complex. There are two effects. First, due to the strong mixing between the s-like A_1 and p-like T_2 states of the three isolated defects, the triplet complex, in general, has energy levels which are very different from those of either the isolated impurity or the vacancy-impurity pair. Secondly, the π-like e levels of the vacancy-impurity pair are split due to the presence of the second impurity which perturbs them. Stated another way, when a second impurity is added to the complex, the C_{3v} symmetry of the pair is reduced to C_{2v} symmetry. Since the point group C_{2v} has one-dimensional irreducible representations only,[35] each energy level associated with a triplet complex is nondegenerate, so that this causes the doubly degenerate e-symmetric levels belonging to the pair to split. Since this splitting is small[15] (≤ 0.2 eV in most cases) and since the b_2-symmetric levels are therefore very similar to both the T_2-symmetric levels of the appropriate impurity and the e-symmetric levels of the pair,[14] results for them are not presented here.

B. Results for specific materials and possible relation to experiment

An interesting phenomenon occurs in the case of the vacancylike a_1-symmetric levels for the anion vacancy complexed with two cation impurities in GaSb, AlP, and AlAs [see Figs. 4(b), 5(b), and 6(b)]; the predicted curves for these levels have two hyperbolalike branches in the band gap, one attached to the conduction band and the other attached to the valence band. This is a consequence of Rayleigh's interlacing theorem,[36,37] which requires that perturbed levels of the same symmetry lie between unperturbed levels. Although this theorem strictly applies for a single defect potential on each atom (the present case has two defect potentials, s and p), the above phenomenon can be qualitatively understood using the following reasoning. For these materials, the A_1-symmetric, isolated anion-vacancy level lies in the band gap. Also, an isolated cation-site impurity which is more electronegative than the atom it replaces will pull a deep level from the conduction band into the band gap. However, when the vacancy is complexed with two identical impurities, this impurity level is prevented from crossing the A_1-symmetric anion-vacancy level by the interlacing theorem. As a result, the conduction-band-attached hyperbola saturates, for large negative potential, to an energy slightly above the isolated anion-vacancy level. In this saturation region, this level has changed from predominantly impuritylike to predominantly vacancylike. At the same time, a vacancylike level has reappeared in a continuous fashion in the lower, valence-band-attached hyperbola.

1. Detailed results for AlP

A brief discussion of the predictions for specific triplet complexes in a representative material is useful for obtaining a general understanding of the effect of complexing two impurities with a vacancy. In fact, many of the features of the deep levels associated with particular complexes in particular materials hold qualitatively from complex to complex and from material to material. Furthermore, comparisons of the triplet-complex-associated levels with the corresponding isolated impurity[7,24] and pair levels[14] show in detail the effects of complexing with a vacancy. For convenience, we consider AlP in some detail. All of our results for the predicted a_1- and b_1-symmetric deep levels associated with triplet complexes in AlP are illustrated in Fig. 5. Figures 5(a) and 5(b), respectively, show results for triplet complexes containing cation and anion vacancies.

Consider first the a_1 and b_1 levels associated with cation vacancy complexes [Fig. 5(a)]. Comparison of our predicted triplet-complex levels with those of the isolated impurities[7,24] or the corresponding vacancy-impurity pair[14] shows that the triplet levels can be very different from those due to either of these defects. An interesting complex to consider is the one containing oxygen, substitutional for P. From Fig. 5(a) it can be seen that the isolated P-site O impurity, as predicted by Hjalmarson *et al.*,[7,24] should produce an A_1 level deep in the band gap (~ 0.5 eV below the conduction-band edge). The impuritylike a_1 and b_1 levels associated with the triplet complex containing O, however, are predicted to be considerably nearer to the conduction band (~ 0.13 eV below the band edge) and almost degenerate. There are two impuritylike levels in this case because there are two impurities. Complexing with a vacancy therefore considerably perturbs the isolated A_1 impurity levels and pushes them much closer to the conduction-band edge. Similar statements can be made about the isolated impurity and triplet-complex levels associated with F and Cl substitutional for P. From Fig. 5(a) it can be seen that P-site impurities Br, N, S, Se, and I should form A_1 levels as isolated impurities.[7,24] When they are part of a triplet complex associated with the Al vacancy, however, the impuritylike a_1 and b_1 levels are pushed out of the gap to become resonant with the conduction band. Inspection of Fig. 5(a) also shows that one member of the Al vacancy T_2 manifold is drastically perturbed by complexing with the P-site impurities At through Tl (reading from left to right at the top of the figure). The resulting a_1 vacancylike levels move from near the bottom of the gap (for At) to near the top (for Tl). A final prediction of Fig. 5(a) is that, although the P-site impurities Zn, Cd, and Hg are predicted to produce no deep levels in the band gap as isolated impurities,[7,24] they should produce b_1 levels near the valence-band edge as part of an Al-vacancy-associated triplet complex.

Similar predictions can be made for the P-vacancy-associated triplet complexes by a detailed examination of Fig. 5(b), which shows that complexing two identical impurities with a P vacancy gives rise to deep levels which are very different from those due either to the pair[14] or the isolated impurity.[7,24] Reading from left to right at the top of Fig. 5(b), the triplet complex for the Al-site impurity F is predicted to produce four deep levels in the band gap (one a_1 impuritylike, one b_1 hybrid, one a_1 hybrid, and one a_1 vacancylike). Similarly, the complexes containing the impurities O, Cl, Br, and N, are predicted

to produce five deep levels (one vacancylike, two impuritylike, and one hybrid), and the triplet complexes containing S through Po are predicted to produce four deep levels in the band gap. Predictions can similarly be obtained for the triplet complexes containing all of the impurities illustrated in the figure.

2. *Deep acceptorlike levels in Ge: Comparison with data*

Two deep hole-trapping states have been observed at 0.23 eV (Ref. 38) and 0.38 eV (Ref. 38) above the valence-band edge in p-type Ge. The experimental techniques used were γ irradiation and quenching from high temperatures. The former level has been attributed to an oxygen-vacancy complex.[38] Our predictions for the deep levels due to the triplet vacancy-oxygen complex in Ge are in qualitative agreement with those data.

Figure 3 contains our predictions for this complex. That figure, and extrapolations of it, show that this defect should produce one b_1 and three a_1 levels resonant with the valence band, one b_1 level near the valence-band edge, one impuritylike a_1 level at 0.2 eV above the valence-band edge, and one a_1 conduction-band-resonant level. Also, the results for the b_2 levels (not shown here; they are similar to the e levels of Ref. 14) give two b_2 levels at 0.5 and 0.7 eV above the valence-band edge.[15] The energy of the impuritylike a_1 level at 0.2 eV agrees with the first of the observed levels to within the accuracy of the theory. Furthermore, this complex in the neutral charge state should contain eight excess electrons. This number is arrived at by noting that when a vacancy replaces a Ge atom, four electrons remain behind to preserve lattice neutrality. When a Ge atom is replaced by an O atom, two extra electrons are contributed. Thus, in undoped material, the four valence-band-resonant levels are each doubly occupied, the b_1 level just near the valence-band edge is empty, and the a_1 level at 0.2 eV is empty (this should be true even in p-type material) and thus observable in the experiments.

On this basis, we conclude that our theory supports the identification of the deep level observed at 0.23 eV with the triplet vacancy-oxygen complex in Ge, and we predict that this level should be of the a_1 type. It is worth noting in passing that neither the vacancy-oxygen pair[14] nor the isolated oxygen impurity[7,24] in Ge are predicted to produce a deep level near 0.2 eV. We also speculate that the observed level near 0.4 eV may be due to this same complex, corresponding to our predicted 0.5-eV b_2 level. Shifts in the predicted levels due to the neglected charge-state splitting and level-occupancy effects could, of course, alter this assignment.

3. *Chlorine A center in ZnSe*

Optically detected magnetic resonance (ODMR) experiments have observed two deep levels at $\sim$0.5 and $\sim$0.6 eV above the valence-band edge in n-type ZnSe.[22,39] These levels have been attributed to a Zn vacancy complexed with Cl (the chlorine A center) and with an unknown impurity, respectively. Our predictions for the triplet complex associated with the Zn vacancy and two Cl neighbors are in qualitative agreement with the data on the 0.5-eV level. Extrapolation of the levels predicted in Fig. 10(a) shows that this complex should produce two impuritylike b_1 levels deep in the valence band, a vacancylike a_1 level just below the valence-band edge, and a vacancylike a_1 level just above the valence-band edge. Furthermore, our results for the b_2 levels associated with this complex predict a level at about 0.4 eV above the valence-band edge.[14,15] By arguments similar to those discussed above, this complex should contain eight excess electrons. Thus, in, undoped material, the valence-band-resonant b_1 and a_1 levels just above the valence-band edge should all be doubly occupied, and the b_2 level should be empty. In n-type material, however, this level could be singly occupied and thus detectable in the ODMR experiments. We conclude that our theory lends support to identification of the deep level observed at 0.5 eV with the complex containing the Zn vacancy and Cl. This is consistent with the data analysis of Ref. 22 and 39.

Referring again to Fig. 10(a) (as well as to Ref. 14 for b_2-level predictions), it is reasonable to speculate that the unknown impurity which, when complexed with a Zn vacancy, gives rise to the observed deep level near 0.6 eV might be I, which was present in some of the samples on which measurements are reported in Refs. 22 and 39.

4. *Zinc-vacancy–chlorine complex in ZnTe*

A deep level observed in photoluminescence at 0.15 eV above the valence-band edge in high-purity ZnTe has been associated with a Zn-vacancy–Cl complex.[21] Furthermore, experimental analysis[21] indicates that the vacancy in this case is doubly positively charged. Our predictions for the deep levels produced by the triplet complex associated with the Zn vacancy and two Cl atoms are very similar to those for the analogous complex ZnSe just discussed. It can be seen from Fig. 11(a) and by electron counting that, in undoped material, this complex should produce two doubly occupied impuritylike b_1 levels deep in the valence band, two doubly occupied vacancylike a_1 levels just below the valence-band edge, and an empty vacancylike b_2 level at 0.5 eV above the valence-band edge.[14,15] We thus conclude that it is reasonable to identify the observed level with our predicted b_2 level. The discrepancy between experimental and theory in this case might be due to charge-state splittings, charge-transfer effects, and lattice relaxation, all of which are negelcted in the present simple approach.

IV. SUMMARY AND CONCLUSIONS

In summary, we have calculated the deep levels associated with triplet complexes in 10 semiconductors. In developing our formalism, we have adopted the framework introduced by Myles and Sankey[14] for the extension of the theory of Hjalmarson *et al.*[7] to treat vacancy-impurity pairs and have further generalized this approach to treat triplet complexes. We again stress that

our theory has ignored lattice relaxation and charge-state splittings. Our results should thus be viewed as the predictions of the global chemical trends of deep levels rather than the predictions of their absolute energies.

One of the primary findings of this work is that a triplet complex may have deep levels which are significantly different from those of either the vacancy-impurity pair[14] or the isolated impurity.[7,24] While this is not profound or surprising, our formalism provides a means of estimating the changes in these levels as the defect is changed from the isolated impurity to the pair to the triplet complex. We hope that our predictions will be useful in assisting in the identification of the defects which produce observed deep levels in the materials considered.

Finally, it is worth pointing out that the formalism developed here is general enough to treat a complex consisting either of three impurities or of an impurity plus a divacancy. However, here, we have limited our predictions to deep levels associated with a vacancy plus two identical impurities. Predictions of deep levels associated with other types of complexes will be presented elsewhere.[40]

ACKNOWLEDGMENTS

It is a pleasure to acknowledge stimulating conversations with E. G. Bylander, R. E. Allen, H. P. Hjalmarson, M. A. Gundersen, and O. F. Sankey. We thank the U.S. National Science Foundation for a grant (No. ECS-84-07185) which supported this work in this early stages, and Texas Tech University for a grant of computer time to perform these calculations. One of us (Y.-T.S.) thanks Texas Tech University for financial support from the Odetta Greer and J. Fred Bucy Endowment for Applied Physics.

APPENDIX: BLOCK DIAGONALIZATION OF THE HOST GREEN'S FUNCTION

In the zinc-blende coordinate system illustrated in Fig. 1, the 12×12 matrix for the Green's function of the perfect crystal has the schematic form

$$G^0(E)=\begin{bmatrix} G^{aa} & G^{ac}(1) & G^{aa}(1,2) \\ G^{ca}(1) & G^{cc} & G^{ca}(2) \\ G^{aa}(2,1) & G^{ac}(2) & G^{aa} \end{bmatrix}, \tag{A1}$$

where the labels a and c refer to anion and cation, where 1 and 2 refer to anion numbers 1 and 2 in Fig. 1, and where we have defined the 4×4 submatrices

$$G^{aa}=\begin{bmatrix} G^{aa}_{ss} & 0 & 0 & 0 \\ 0 & G^{aa}_{xx} & 0 & 0 \\ 0 & 0 & G^{aa}_{xx} & 0 \\ 0 & 0 & 0 & G^{aa}_{xx} \end{bmatrix}, \tag{A2}$$

$$G^{ca}(1)=\begin{bmatrix} G^{ca}_{ss}(1) & G^{ca}_{sx}(1) & G^{ca}_{sy}(1) & G^{ca}_{sz}(1) \\ G^{ca}_{xs}(1) & G^{ca}_{xx}(1) & G^{ca}_{xy}(1) & G^{ca}_{xz}(1) \\ G^{ca}_{ys}(1) & G^{ca}_{yx}(1) & G^{ca}_{yy}(1) & G^{ca}_{yz}(1) \\ G^{ca}_{zs}(1) & G^{ca}_{zx}(1) & G^{ca}_{zy}(1) & G^{ca}_{zz}(1) \end{bmatrix}, \tag{A3}$$

and

$$G^{aa}(2,1)=\begin{bmatrix} G^{aa}_{ss}(2,1) & G^{aa}_{sx}(2,1) & G^{aa}_{sy}(2,1) & G^{aa}_{sz}(2,1) \\ G^{aa}_{xs}(2,1) & G^{aa}_{xx}(2,1) & G^{aa}_{xy}(2,1) & G^{aa}_{xz}(2,1) \\ G^{aa}_{ys}(2,1) & G^{aa}_{yx}(2,1) & G^{aa}_{yy}(2,1) & G^{aa}_{yz}(2,1) \\ G^{aa}_{zs}(2,1) & G^{aa}_{zx}(2,1) & G^{aa}_{zy}(2,1) & G^{aa}_{zz}(2,1) \end{bmatrix}. \tag{A4}$$

The submatrix G^{cc} has the same form as G^{aa} with the replacement of the label a by label c, and the submatrix $G^{ca}(2)$ has the same form as $G^{ca}(1)$ with the replacement of the label 1 by the label 2. Also, in the energy gap, $G^0(E)$ is a real symmetric matrix. We therefore have

$$G^{ac}(1)=[G^{ca}(1)]^T,$$

$$G^{ac}(2)=[G^{ca}(2)]^T,$$

$$G^{aa}(1,2)=[G^{aa}(2,1)]^T,$$

where T means the transpose of the matrix.

The matrix elements in Eqs. (A2)–(A4) are written in suggestive notation. They are defined in the atomiclike basis discussed earlier as, for example,

$$G^{ca}_{sx}(1)=\langle sc\mathbf{0}|(E-H_0)^{-1}|p_x a\mathbf{d}\rangle, \tag{A5}$$

$$G^{ca}_{sx}(2)=\langle sc\mathbf{0}|(E-H_0)^{-1}|p_x a\mathbf{d}'\rangle, \tag{A6}$$

$$G^{aa}_{sx}(2,1)=\langle sa\mathbf{d}'|(E-H_0)^{-1}|p_x a\mathbf{d}\rangle, \tag{A7}$$

with similar definitions for the rest of the matrix elements. (The subscripts x, y, and z refer to the three p orbitals p_x, p_y, and p_z.)

After using the symmetric operations of the point group C_{2v},[35] the 12×12 Green's function G^0, Eq. (A1), can algebraically be block-diagonalized into the direct sum of four smaller matrices. The proof of this is quite lengthy and is shown in detail in the Appendix of Ref. 15.

The result of this manipulation is

$$G^0(E)=\begin{bmatrix} G^0_5 & 0 & 0 & 0 \\ 0 & G^0_4 & 0 & 0 \\ 0 & 0 & G^0_2 & 0 \\ 0 & 0 & 0 & G^0_1 \end{bmatrix}, \tag{A8}$$

where G^0_5, G^0_4, and G^0_2 are, respectively, 5×5, 4×4, and 2×2 matrices, and G^0_1 is a scalar. The explicit expressions for the smaller submatrices shown schematically in Eq. (A8) can be written as follows.[15] The 5×5 submatrix has the form

$$G_5^0=\begin{bmatrix} G_5^0(1,1) & G_5^0(1,2) & G_5^0(1,3) & G_5^0(1,4) & G_5^0(1,5) \\ G_5^0(1,2) & G_5^0(2,2) & G_5^0(2,3) & G_5^0(2,4) & 0 \\ G_5^0(1,3) & G_5^0(2,3) & G_5^0(3,3) & G_5^0(3,4) & G_5^0(3,5) \\ G_5^0(1,4) & G_5^0(2,4) & G_5^0(3,4) & G_5^0(4,4) & G_5^0(4,5) \\ G_5^0(1,5) & 0 & G_5^0(3,5) & G_5^0(4,5) & G_5^0(5,5) \end{bmatrix}, \tag{A9}$$

where we have defined

$$G_5^0(1,1)=G_{ss}^{aa}+G_{ss}^{aa}(2,1),\quad G_5^0(2,2)=G_{ss}^{cc},\quad G_5^0(3,3)=G_{xx}^{aa}-G_{xx}^{aa}(2,1)-G_{xy}^{aa}(2,1),$$
$$G_5^0(4,4)=G_{xx}^{aa}+G_{zz}^{aa}(2,1),\quad G_5^0(5,5)=G_{xx}^{cc},\quad G_5^0(1,2)=\sqrt{2}G_{ss}^{ca},$$
$$G_5^0(1,3)=-\sqrt{2}G_{sx}^{aa}(2,1),\quad G_5^0(1,4)=G_{sz}^{aa}(2,1),\quad G_5^0(1,5)=\sqrt{2}G_{xs}^{ca},$$
$$G_5^0(2,3)=-2G_{sx}^{ca},\quad G_5^0(2,4)=\sqrt{2}G_{xz}^{aa}(2,1),\quad G_5^0(3,4)=\sqrt{2}G_{xz}^{aa}(2,1),$$
$$G_5^0(3,5)=-2G_{xy}^{ca},\quad G_5^0(4,5)=\sqrt{2}G_{xx}^{ca}.$$

The 4×4 submatrix has the form

$$G_4^0=\begin{bmatrix} G_4^0(1,1) & G_4^0(1,2) & G_4^0(1,3) & G_4^0(1,4) \\ G_4^0(1,2) & G_4^0(2,2) & G_4^0(2,3) & G_4^0(2,4) \\ G_4^0(1,3) & G_4^0(2,3) & G_4^0(3,3) & G_4^0(3,4) \\ G_4^0(1,4) & G_4^0(2,4) & G_4^0(3,4) & G_4^0(4,4) \end{bmatrix}, \tag{A10}$$

where we have defined

$$G_4^0(1,1)=G_{ss}^{aa}-G_{ss}^{aa}(2,1),\quad G_4^0(2,2)=G_{xx}^{aa}+G_{xx}^{aa}(2,1)+G_{xy}^{aa}(2,1),$$
$$G_4^0(3,3)=G_{xx}^{cc},\quad G_4^0(4,4)=G_{xx}^{aa}-G_{zz}^{aa}(2,1),\quad G_4^0(1,2)=\sqrt{2}G_{sx}^{aa}(2,1),$$
$$G_4^0(1,3)=-2G_{xs}^{ca},\quad G_4^0(1,4)=-G_{sz}^{aa}(2,1),\quad G_4^0(2,3)=\sqrt{2}(G_{xx}^{ca}+G_{xy}^{ca}),$$
$$G_4^0(2,4)=-\sqrt{2}G_{xz}^{aa}(2,1),\quad G_4^0(3,4)=-2G_{xy}^{xa}.$$

The 2×2 submatrix has the form

$$G_2^0=\begin{bmatrix} G_2^0(1,1) & G_2^0(1,2) \\ G_2^0(1,2) & G_2^0(2,2) \end{bmatrix}, \tag{A11}$$

where we have defined

$$G_2^0(1,1)=G_{xx}^{aa}+G_{xx}^{aa}(2,1)-G_{xy}^{aa}(2,1),$$
$$G_2^0(2,2)=G_{xx}^{cc},$$

and

$$G_2^0(1,2)=\sqrt{2}(G_{xx}^{ca}-G_{xy}^{ca}).$$

Finally, the 1×1 or scalar part of the Green's function has the form

$$G_1^0=G_1^0(1,1)=G_{xx}^{aa}-G_{xx}^{aa}(2,1)+G_{xy}^{aa}(2,1). \tag{A12}$$

In writing these expressions, we have used the shorthand notation

$$G_{ss}^{ca}=G_{ss}^{ca}(1),\quad G_{xx}^{ca}=G_{xx}^{ca}(1),$$
$$G_{sx}^{ca}=G_{sx}^{ca}(1),\quad G_{xs}^{ca}=G_{xs}^{ca}(1),$$

and

$$G_{xy}^{ca}=G_{xy}^{ca}(1).$$

The defect potential is diagonal, as is discussed in the text. It can thus be written as the direct sum

$$U=U_5+U_4+U_2+U_1, \tag{A13}$$

where U_i, $i=5,4,2$, are $i\times i$ submatrices and U_1 is a scalar. These have the form

$$U_5=\begin{bmatrix} U_s^a & 0 & 0 & 0 & 0 \\ 0 & U_s^c & 0 & 0 & 0 \\ 0 & 0 & U_p^a & 0 & 0 \\ 0 & 0 & 0 & U_p^a & 0 \\ 0 & 0 & 0 & 0 & U_p^c \end{bmatrix}, \tag{A14}$$

$$U_4=\begin{bmatrix} U_p^a & 0 & 0 & 0 \\ 0 & U_p^a & 0 & 0 \\ 0 & 0 & U_p^c & 0 \\ 0 & 0 & 0 & U_p^a \end{bmatrix}, \tag{A15}$$

$$U_2 = \begin{bmatrix} U_p^a & 0 \\ 0 & U_p^c \end{bmatrix}, \tag{A16}$$

and

$$U_1 = U_p^a . \tag{A17}$$

Finally, by combining Eq. (A8) with Eq. (A13), it can be shown that the 12×12 Koster-Slater eigenvalue determinant factors to become Eq. (5) of the text.

---

*Present address: Zeeman Laboratory, University of Amsterdam, 1018 TV, Amsterdam, The Netherlands.

[1]See, for example, W. Kohn, in *Solid State Physics,* edited by F. Seitz and D. Turnbull (Academic, New York, 1957), Vol. 5, Chap. 4, and references therein.

[2]S. T. Pantelides, Rev. Mod. Phys. **50**, 797 (1978).

[3]M. Jaros, *Deep Levels in Semiconductors* (Hilger, Bristol, 1982); Adv. Phys. **29**, 409 (1980).

[4]G. A. Baraff and M. Schlüter, Phys. Rev. Lett. **41**, 892 (1978).

[5]J. Bernholc, N. O. Lipari, and S. T. Pantelides, Phys. Rev. Lett. **41**, 895 (1978).

[6]L. A. Hemstreet, Phys. Rev. B **15**, 834 (1977).

[7]H. P. Hjalmarson, P. Vogl, D. J. Wolford, and J. D. Dow, Phys. Rev. Lett. **44**, 810 (1980).

[8]G. F. Koster and J. C. Slater, Phys. Rev. **95**, 1167 (1954).

[9]O. F. Sankey, H. P. Hjalmarson, J. D. Dow, D. J. Wolford, and B. G. Streetman, Phys. Rev. Lett. **45**, 1656 (1980).

[10]O. F. Sankey and J. D. Dow, Appl. Phys. Lett. **38**, 685 (1981).

[11]O. F. Sankey and J. D. Dow, J. Appl. Phys. **52**, 5139 (1981).

[12]J. D. Dow, R. E. Allen, O. F. Sankey, J. P. Buisson, and H. P. Hjalmarson, J. Vac. Sci. Technol. **19**, 502 (1981).

[13]O. F. Sankey and J. D. Dow, Phys. Rev. B **26**, 3243 (1982).

[14]C. W. Myles and O. F. Sankey, Phys. Rev. B **29**, 6810 (1984).

[15]Y.-T. Shen, Ph.D. dissertation, Texas Tech University, Lubbock, TX, 1986. A more exhaustive discussion of the theory presented here and of the major results may be found in this reference.

[16]Y.-T. Shen and C. W. Myles, Appl. Phys. Lett. **51**, 2304 (1987); J. Appl. Phys. **65**, 4273 (1989).

[17]A. O. Evwaraye, J. Appl. Phys. **48**, 1840 (1977).

[18]R. N. Bhargava, S. K. Kurtz, A. T. Vink, and R. C. Peters, Phys. Rev. Lett. **27**, 183 (1971).

[19]V. I. Vovenka, K. D. Glinchuk, and A. V. Prokhorovich, Fiz. Tekh. Poluprovdn. **10**, 2167 (1976) [Sov. Phys.—Semicond. **10**, 1288 (1976)].

[20]E. G. Bylander (unpublished).

[21]T. Taguchi, Phys. Status Solidi B **96**, K33 (1976).

[22]D. J. Dunstan, J. E. Nicholls, B. C. Cavenett, and J. J. Davies, J. Phys. C **13**, 6409 (1980).

[23]C. W. Myles, P. F. Williams, R. A. Chapman, and E. G. Bylander, J. Appl. Phys. **57**, 5279 (1985).

[24]H. P. Hjalmarson, Ph.D. dissertation, University of Illinois at Urbana-Champaign, Urbana, IL, 1979.

[25]P. Vogl, H. P. Hjalmarson, and J. D. Dow, J. Phys. Chem. Solids **44**, 365 (1983).

[26]W. C. Ford, C. W. Myles, and R. L. Lichti, Phys. Rev. B **38**, 10533 (1988); W. C. Ford and C. W. Myles, *ibid.* **38**, 1210 (1988); **34**, 927 (1986); C. W. Myles and W. C. Ford, J. Vac. Sci. Technol. A **4**, 2195 (1986); W. C. Ford, Ph.D. dissertation, Texas Tech University, Lubbock, TX 1986.

[27]H. H. Dai, M. A. Gundersen, C. W. Myles, and P. G. Snyder, Phys. Rev. B **37**, 1205 (1988); H. H. Dai, M. A. Gundersen, and C. W. Myles, *ibid.* **33**, 8234 (1986).

[28]See, for example, S. Lee, J. D. Dow, and O. F. Sankey, Phys. Rev. B **31**, 3910 (1985), where charge-state splittings are incorporated into the theory of Hjalmarson *et al.* (Refs. 7 and 24) and results are compared with the results of J. Bernholc, N. O. Lipari, S. T. Pantelides, and M. Scheffler, Phys. Rev. B **26**, 5706 (1982).

[29]R. E. Allen, T. S. Humphreys, J. D. Dow, and O. F. Sankey, J. Vac. Sci. Technol. B **2**, 449 (1984); C. W. Myles, S.-F. Ren, R. E. Allen, and S.-Y. Ren, Phys. Rev. B **35**, 9758 (1987), and references therein.

[30]We define an ideal vacancy in a manner identical to that used in other empirical tight-binding schemes. That is, an atom is removed from the perfect crystal, leaving all other atoms at their original positions. The atomiclike orbitals are retained on all other atoms and their interactions are assumed unaltered. This assumption has been shown to be equivalent to the "bond-cutting" method of creating an ideal vacancy. See, for example, S. Das Sarma and A. Madhukar, Phys. Rev. B **24**, 2051 (1981).

[31]J. R. Chelikowsky and M. L. Cohen, Phys. Rev. B **14**, 556 (1976).

[32]W. A. Harrison, *Electronic Structure and the Properties of Solids* (Freeman, San Francisco, 1980). Both the on-site and transfer-matrix elements of H_0 (Ref. 25) are constructed in the spirit of Harrison's universal model.

[33]Following earlier work, we assume that the defect potential of the s^* orbital vanishes.

[34]Such differences are similar to electronegativity differences used by J. C. Phillips, Phys. Rev. B **1**, 1540 (1970).

[35]M. Tinkman, *Group Theory and Quantum Mechanics* (McGraw-Hill, New York, 1964).

[36]See, for example, A. A. Maradudin, E. W. Montroll, and G. H. Weiss, in *Solid State Physics,* edited by F. Seitz, D. Turnbull, and H. Ehrenreich (Academic, New York, 1963), Suppl. 3, p. 132.

[37]For this theorem to be rigorously applicable, one must fix the p atomic energy of the impurity at the host value and permit only the s atomic energy to vary. See Ref. 9.

[38]S. J. Pearton, A. J. Tavendale, J. M. Kahn, and E. E. Haller, Radiat. Eff. **81**, 293 (1984); S. J. Pearton, E. E. Haller, and J. M. Kahn, J. Phys. C **17**, 2375 (1984).

[39]K. M. Lee, L. S. Dang, and G. D. Watkins, Solid State Commun. **35**, 527 (1980).

[40]W.-G. Li, C. W. Myles, and Y.-T. Shen, Phys. Rev. B (to be published).